Quadrupole Deformation of the Self-Conjugate Nucleus ^{72}Kr

A. Gade,[1] D. Bazin,[1] A. Becerril,[1,2] C. M. Campbell,[1,2] J. M. Cook,[1,2] D. J. Dean,[3] D.-C. Dinca,[1,2] T. Glasmacher,[1,2] G. W. Hitt,[1,2] M. E. Howard,[4] W. F. Mueller,[1] H. Olliver,[1,2] J. R. Terry,[1,2] and K. Yoneda[1]

[1]*National Superconducting Cyclotron Laboratory, Michigan State University, East Lansing, Michigan 48824, USA*
[2]*Department of Physics and Astronomy, Michigan State University, East Lansing, Michigan 48824, USA*
[3]*Physics Division, Oak Ridge National Laboratory, Oak Ridge, Tennessee 37831, USA*
[4]*Department of Physics, The Ohio State University, Columbus, Ohio 43210, USA*

(Received 7 February 2005; published 7 July 2005)

We report on the first determination of the absolute $B(E2; 0_1^+ \rightarrow 2_1^+)$ excitation strength in the $N = Z$ nucleus ^{72}Kr. ^{72}Kr is the heaviest $N = Z$ nucleus for which this quantity has been measured and provides a benchmark in a region of the nuclear chart dominated by rapidly changing deformations and shapes mediated by the interplay of strongly oblate and prolate-driving orbitals. The deduced quadrupole deformation strength is in agreement with a variety of self-consistent models that predict an oblate shape for the ground state of ^{72}Kr. Large-scale shell-model Monte Carlo calculations reproduce the experimental $B(E2)$ value and link the result to the occupation of the deformation-driving $g_{9/2}$ orbit.

DOI: 10.1103/PhysRevLett.95.022502 PACS numbers: 21.10.Ft, 25.70.De, 25.70.Mn, 27.50.+e

The shape of the atomic nucleus is determined by the interplay of macroscopic and microscopic effects within this quantum mechanical many-body system. The even-even self-conjugate nuclei with $28 \leq N = Z \leq 50$ are of particular interest. The fp shell with the deformation-driving $g_{9/2}$ orbital is large enough for these nuclei to exhibit all aspects of collective behavior including a remarkable diversity of shapes, sizable ground-state deformations, triaxiality, and the coexistence of oblate and prolate shapes at low excitation energy. These effects are generally assessed to be caused by the occurrence of well pronounced, *deformed* shell gaps in the Nilsson diagram, amplified by the simultaneous occupancy of identical orbitals by valence protons *and* neutrons. The ground-state shape along the $N = Z$ line in the nuclear chart is supported by limited experimental information and is predicted to change from triaxial (^{64}Ge), oblate (^{68}Se, ^{72}Kr), strongly prolate (^{76}Sr, ^{80}Zr), to spherical (^{84}Mo) as $N = Z$ increases [1,2]. Enhanced proton-neutron correlations in self-conjugate nuclei are discussed extensively and controversially in the literature [3,4]; however, the manifestation and signatures of *proton-neutron pairing* are still under debate.

For ^{72}Kr, excitation energies, band structures up to spin values of $28\hbar$, and the changes in shape with increased rotational frequencies have been investigated in fusion-evaporation reactions induced by stable beams, employing first-generation γ-ray detector systems [5] and the large, multidetector γ-ray spectrometers GAMMASPHERE, GASP, and EUROBALL [6–8]. Recently, ^{72}Kr has been studied with the combination of conversion-electron and γ-ray spectroscopy following fast fragmentation of a ^{78}Kr beam at Grand Accelerateur National D'Ions Lourds (GANIL) [9]. An isomeric 0^+ state could be established as the first excited state and has been interpreted as the bandhead of a previously known rotational structure with prolate deformation [9]. The measured electric monopole $E0$ transition strength between the excited 0^+ state and the ground state, which indicates a change in the mean square radius of the nucleus in those configurations, provides experimental evidence for the phenomenon of shape coexistence with the ground state of ^{72}Kr suggested as almost purely oblate deformed [9]. In spite of the combination of the two aforementioned complementary nuclear-spectroscopy techniques utilizing the unique capabilities of stable and radioactive beam facilities, the very fundamental information on the *size* of the quadrupole deformation of the ground state of ^{72}Kr remains unavailable.

The radius of a quadrupole-deformed nucleus can be expressed in terms of spherical harmonics of second order with the expansion coefficients parametrized by the quadrupole deformation strength β and the asymmetry angle γ [10]. In the convention used by [11], $\beta > 0$ with the asymmetry angle $0° \leq \gamma \leq 60°$ characterizing oblate ($\gamma = 60°$), prolate ($\gamma = 0°$), or triaxial shapes ($0° \neq \gamma \neq 60°$). The absolute $B(E2; 0_1^+ \rightarrow 2_1^+) = B(E2\uparrow)$ quadrupole excitation strength of an even-even nucleus with mass and charge numbers A and Z relates to the size of the deformation β via [12]

$$\beta = \frac{4\pi}{3ZR_0^2}\sqrt{B(E2\uparrow)/e^2}, \qquad R_0 = 1.2A^{1/3}\ \mathrm{fm}. \tag{1}$$

The availability of fast exotic beams prompted the development of intermediate-energy Coulomb excitation as a technique to measure the $B(E2\uparrow)$ value in even-even nuclei very far from stability with low beam rates and thick targets [13]. Exotic nuclei are scattered off stable high-Z targets and are detected in coincidence with the deexcitation γ rays tagging the inelastic process (see, for example, [14–18]). Very peripheral collisions are selected experimentally in the regime of intermediate-energy beams to exclude nuclear contributions to the electromagnetic excitation process. This can be accomplished by restricting the analysis to events at extremely forward scattering angles, corresponding to large impact parameters for the collision between beam particles and target nuclei. This method has been extensively compared to measurements at low beam energies and is well established (see [13] and references within).

Here, we report on the first measurement of the absolute $B(E2\uparrow)$ excitation strength in $^{72}Kr_{36}^{36}$. The present intermediate-energy Coulomb excitation experiment was performed at the Coupled Cyclotron Facility of the National Superconducting Cyclotron Laboratory at Michigan State University.

The secondary beam cocktail containing ^{72}Kr was produced by fragmentation of a 140 MeV/nucleon ^{78}Kr primary beam impinging on a 329 mg/cm^2 ^9Be fragmentation target in the A1900 fragment separator [19]. A ^{197}Au target of 184(4) mg/cm^2 thickness was placed at the target position of the S800 magnetic spectrograph [20], which identifies scattered particle species. The target was surrounded by sixteen 32-fold segmented HPGe detectors (SeGA) [21] to measure photon energies and their emission angles. The detectors were arranged at a distance of 24 cm from the target in two rings with central angles of 90° (nine detectors) and 37° (seven detectors) relative to the beam axis. The photopeak efficiency of the array was corrected for the Lorentz boost of the photon distribution emitted by fast moving projectiles, for the γ-ray angular distribution following Coulomb excitation [22], as well as for absorption effects in the gold target. An accuracy of 6.5% results for the in-beam efficiency.

The particle identification and the determination of the scattering angle off the gold target were performed event by event with the focal-plane detector system of the S800 spectrograph [20]. The energy loss in the ion chamber and time-of-flight information taken between two scintillators were employed to unambiguously identify the particles scattered off the gold target. To obtain separation between the constituents of the cocktail beam, the time-of-flight information was corrected for the particle's flight path through the spectrograph on an event-by-event basis using the angle information from the focal plane and the energy. The ion's energy loss as a function of the time of flight is shown in Fig. 1 without and with the aforementioned corrections. Only 1.7% of the nuclei in the beam cocktail were ^{72}Kr, making the event-by-event tracking of particles crucial for the success of the experiment.

The two position-sensitive cathode readout drift counters of the S800 detector system in conjunction with the known optics of the spectrograph served to reconstruct the scattering angle on an event-by-event basis. The angle-integrated Coulomb excitation cross section $\sigma(\theta_{\rm lab} \le \theta_{\rm lab}^{\rm max})$ is then given by the efficiency-corrected peak area in the γ-ray spectrum relative to the number of particles (with scattering angles $\theta_{\rm lab} \le \theta_{\rm lab}^{\rm max}$) per number density of the target. We used the maximum scattering angles $\theta_{\rm lab}^{\rm max} = 2.5°$ and 3.0° corresponding to two different minimum impact parameters. A systematic uncertainty of 7.6% for $\theta_{\rm lab}^{\rm max} = 2.5°$ and 6.5% at $\theta_{\rm lab}^{\rm max} = 3.0°$ attributed to an 0.1° uncertainty in the scattering-angle reconstruction is considered and added in quadrature. The angle-integrated cross sections are then translated into absolute $B(E2)$ excitation strengths using the Winther-Alder theory of relativistic Coulomb excitation [22].

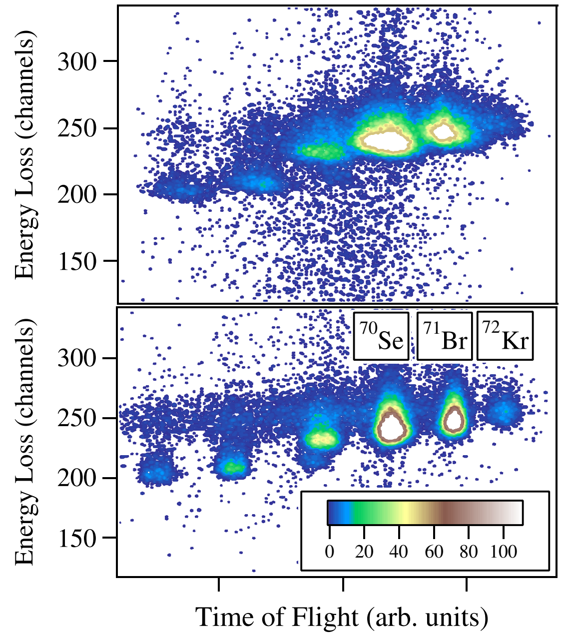

FIG. 1 (color online). Particle-identification spectrum of the cocktail beam containing about 1200 ^{72}Kr nuclei (only 1.7% of the total number of particles in the spectrum). A software gate has been applied to eliminate the hydrogenlike charge state produced in the gold target. The upper panel shows the particle-identification (PID) spectrum without time-of-flight correction, while the spectrum in the lower panel shows the PID spectrum with the time of flight adjusted for the different flight paths for different isotopes as discussed in the text.

Intermediate-energy Coulomb excitation of the primary beam ^{78}Kr served as test case for the experimental approach. The beam was degraded to a midtarget energy of 57.4 MeV/nucleon in the Coulomb excitation target. The electromagnetic interaction is generally assumed to dominate in heavy-ion collisions whenever the minimum impact parameter $b_{\rm min}$ exceeds the electromagnetic interaction radius $R_{\rm int}$ [23]. For the given kinematics, $b_{\rm min}$ corresponding to $\theta_{\rm lab}^{\rm max} = 2.5°$ and 3.0°, are 21.3 and 17.8 fm, respectively, exceeding $R_{\rm int} = 14.07$ fm for the projectile-target system by more than 3 fm. The measured angle-integrated Coulomb excitation cross section $\sigma(\theta_{\rm lab} \le 2.5°) = 783(108)$ mb and $\sigma(\theta_{\rm lab} \le 3.0°) = 1124(133)$ mb translate into absolute $E2$ excitation strength of $B(E2\uparrow) = 6111(839)\ e^2{\rm fm}^4$ and $6244(738)\ e^2{\rm fm}^4$, respectively. The results are consistent with each other and agree with the adopted value of $B(E2\uparrow) = 6330(390)\ e^2{\rm fm}^4$ for ^{78}Kr [12]. The γ-ray spectrum observed in coincidence with the scattered ^{78}Kr beam is shown in the left column of Fig. 2.

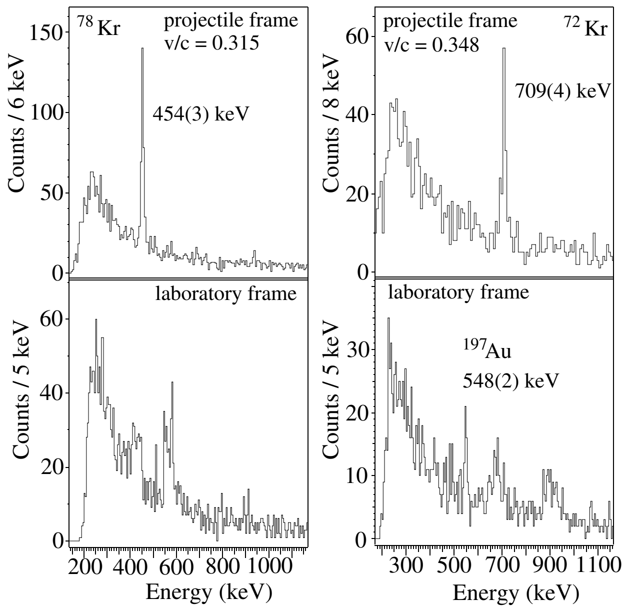

FIG. 2. Intermediate-energy Coulomb excitation of the first 2^+ state of ^{78}Kr (left column) and ^{72}Kr (right column) with the maximum projectile scattering angle restricted to $\theta_{\rm lab}^{\rm max} = 3°$. The spectra show the γ rays observed in the laboratory system (lower panel) and the result of the event-by-event Doppler reconstruction of the data into the projectile reference frame (upper panel).

The γ-ray spectrum detected in coincidence with ^{72}Kr is shown in the right column of Fig. 2. The midtarget energy of the ^{72}Kr beam was 69.3 MeV/nucleon resulting in impact parameters $b_{\rm min}(2.5°) = 19.2$ fm and $b_{\rm min}(3.0°) = 16.0$ fm for the respective maximum scattering angles, well above the electromagnetic interaction radius $R_{\rm int} = 13.95$ fm for the (^{72}Kr, ^{197}Au) system. The absolute excitation strengths $B(E2\uparrow) = 5167(757)\ e^2$fm^4 and $B(E2\uparrow) = 4997(647)\ e^2$fm^4 were deduced [22] from angle-integrated cross sections $\sigma(\theta_{\rm lab} \leq 2.5°) = 696(102)$ mb and $\sigma(\theta_{\rm lab} \leq 3.0°) = 943(122)$ mb, respectively.

Table I summarizes the experimental results for ^{72}Kr and ^{78}Kr. The deformation parameter β, the static quadrupole moment $|Q_0|$, and the mean lifetime τ are deduced from the $B(E2\uparrow)$ values. Prolate and oblate deformed states can be distinguished via the sign of the static quadrupole moment Q_0. In intermediate-energy Coulomb excitation, only the absolute value $|Q_0|$ is accessible. Beam energies near the Coulomb barrier of the projectile-target system would allow for multistep Coulomb excitation processes providing the possibility to determine the sign of the quadrupole moment experimentally [24]. However, the production of a ^{72}Kr beam at low energies with sufficient intensity has not been possible so far.

An exceptional amount of model calculations has been applied to describe the properties of coexisting shapes in ^{72}Kr. Figure 3 compares the experimental quadrupole deformation strength β to the deformation of the lowest oblate and prolate solutions for a variety of self-consistent approaches that predict prolate-oblate shape coexistence [1,2,25–27]. The experimental result of $\beta = 0.330(21)$ and the deformation strength of the oblate minimum predicted within the configuration-dependent shell-correction approach [1], the symmetry-unrestricted Skyrme Hartree-Fock Bogoliubov calculation [2], and relativistic mean-field calculations employing the NL3 and TM1 parameter sets, respectively [25], agree within error bars. The deformation strength of the prolate solution is outside the 1-sigma experimental uncertainty for every model. This strongly supports the assignment of oblate deformation for the ground state of ^{72}Kr, so far solely based on the observation and interpretation of the $E0$ strength measured between the excited 0^+ state and the ground state [9].

In ^{72}Kr, the $g_{9/2}$ orbit is well above the Fermi energy and thus can be interpreted as a particlelike intruder orbital [28]. From the Nilsson scheme, the oblate ground state of ^{72}Kr can be tied to the occupation of the strongly oblate-driving [404]9/2 Nilsson orbit by two protons and neutrons, while in the neighboring isotopes ^{74,76}Kr prolate-driving orbitals are being filled, explaining the rapid changes in shape in this area of the nuclear chart. Though the $B(E2\uparrow)$ strengths is a collective observable, the $B(E2\uparrow)$ value in ^{72}Kr is linked to single-particle structure and occupancy due to the special role of the $g_{9/2}$ orbit.

For further interpretation, we also performed shell-model Monte Carlo (SMMC) [29] calculations in the $0f$-$1p$-$0g$-$1d$-$2s$ oscillator model space. The SMMC

TABLE I. Experimental results for ^{72}Kr and ^{78}Kr compared to the adopted values from [12]. The deformation parameter β, the static quadrupole moment $|Q_0|$, and the mean lifetime τ are deduced from the $B(E2\uparrow)$ strength. For our results, we adopt the values deduced at $\theta_{\rm lab} \leq \theta_{\rm max}^{\rm lab} = 3.0°$ due to higher statistics and resulting smaller uncertainty.

	^{72}Kr	Ref. [12]	^{78}Kr	Ref. [12]
$E(2_1^+)$ (keV)	709(4)	709.1(3)	453(3)	455.8(1)
$\sigma(\theta_{\rm lab} \leq 3.0°)$ (mb)	943(106)		1124(133)	
$B(E2\uparrow)$ (e^2fm^4)	4997(647)	$\cdots$	6244(738)	6330(390)
β	0.330(21)	$\cdots$	0.350(21)	0.352(11)
$\|Q_0\|$ (b)	2.24(14)	$\cdots$	2.51(15)	2.52(8)
τ (ps)	4.53(59)	$\cdots$	33.5(40)	33.0(20)

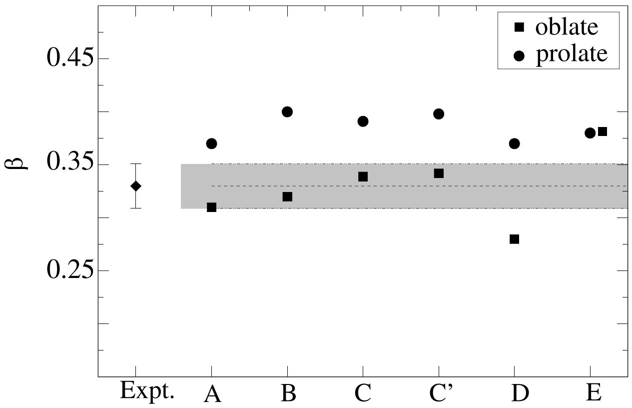

FIG. 3. Experimental results for the quadrupole deformation strength β of ^{72}Kr compared to the lowest prolate and oblate solutions of various self-consistent models predicting shape coexistence (A: configuration-dependent shell-correction approach [1]; B: symmetry-unrestricted Skyrme Hartree-Fock Bogoliubov calculation [2]; C,C$'$: relativistic mean-field calculation with NL3 and TM1 parameter sets, respectively [25]; D: self-consistent adiabatic large-amplitude collective motion [26]; E: large-scale variational approach [27]. The oblate minimum is predicted to be the ground state within all the models.

method calculates expectation values of thermally averaged operators Ω for a given nuclear Hamiltonian through an auxiliary field quantum Monte Carlo technique. For the Hamiltonian, we use a pairing-plus-quadrupole interaction as described in Ref. [28] with appropriately derived pairing and quadrupole strengths, and single-particle energies taken from a Woods-Saxon potential appropriate for ^{56}Ni. The initial single-particle energies are given by (normalized to the $0f_{7/2}$ and in units of MeV): $\varepsilon(0f_{7/2}) = 0.0$, $\varepsilon(0f_{5/2}) = 6.42$, $\varepsilon(1p_{3/2}) = 4.35$, $\varepsilon(1p_{1/2}) = 6.54$, $\varepsilon(0g_{9/2}) = 8.98$, $\varepsilon(0g_{7/2}) = 17.59$, $\varepsilon(1d_{5/2}) = 12.95$, $\varepsilon(1d_{3/2}) = 15.99$, $\varepsilon(2s_{1/2}) = 14.64$. Our SMMC calculations were performed at $1/T = 2.5$ MeV^{-1}. The corresponding β-γ plots (performed as in [30]) for ^{72}Kr suggest that it has a soft oblate ground state. The calculated total $B(E2\uparrow)$ is 5381 ± 31 e^2fm^4 ($\beta = 0.34$, which is slightly larger than, but consistent with, the experimental value obtained in this work). The ground-state occupation of $0g_{9/2}$ is 1.73 ± 0.01 in both protons and neutrons. Variation of the gap between the fp- and gds-major shells significantly alters this picture. Decreasing the gap by 0.25 MeV generates a prolate deformed ground state with $\beta = 0.39$, while increasing the gap by 0.25 MeV generates a nearly gamma-soft nucleus with $\beta = 0.30$. These calculations indicate a delicate balance between the single-particle energy spacings and the oblate character of the ground state.

In summary, we measured the absolute $B(E2\uparrow)$ excitation strength in ^{72}Kr for the first time. ^{72}Kr is the heaviest self-conjugate nucleus for which this quantity has been measured. The deduced quadrupole deformation parameter β of the ^{72}Kr ground state agrees with the oblate solution of a variety of self-consistent models, while prolate solutions consistently lie outside the 1-sigma experimental uncertainty, thus supporting the assignment of oblate deformation for the ground state of ^{72}Kr. A wide variety of experimental techniques at stable and radioactive beam facilities has been applied to investigate ^{72}Kr, and, yet, the direct measurement of the oblate ground-state deformation remains a challenge for future experiments.

We acknowledge stimulating discussions with M. Bender. This work was supported by the National Science Foundation under Grants No. PHY-0110253, No. PHY-9875122, No. PHY-0244453, and No. PHY-0342281, and the U.S. DOE under Contract No. DE-AC05-00OR22725.

[1] W. Nazarewicz *et al.*, Nucl. Phys. **A435**, 397 (1985).
[2] M. Yamagami *et al.*, Nucl. Phys. **A693**, 579 (2001).
[3] W. Satula *et al.*, Phys. Rev. Lett. **87**, 052504 (2001).
[4] A. O. Macchiavelli *et al.*, Phys. Lett. B **480**, 1 (2000).
[5] C. J. Lister *et al.*, Phys. Rev. C **42**, R1191 (1990).
[6] S. M. Fischer *et al.*, Phys. Rev. Lett. **87**, 132501 (2001); N. S. Kelsall *et al.*, Phys. Rev. C **64**, 024309 (2001); S. M. Fischer *et al.*, Phys. Rev. C **67**, 064318 (2003).
[7] G. de Angelis *et al.*, Phys. Lett. B **415**, 217 (1997).
[8] S. Skoda *et al.*, Phys. Rev. C **58**, R5 (1998).
[9] E. Bouchez *et al.*, Phys. Rev. Lett. **90**, 082502 (2003).
[10] D. L. Hill and J. A. Wheeler, Phys. Rev. **89**, 1102 (1953).
[11] P. Ring and P. Schuck, *The Nuclear Many-Body Problem* (Springer-Verlag, Berlin, 2000), p. 5.
[12] S. Raman *et al.*, At. Data Nucl. Data Tables **78**, 1 (2001).
[13] T. Glasmacher, Annu. Rev. Nucl. Part. Sci. **48**, 1 (1998).
[14] T. Motobayashi *et al.*, Phys. Lett. B **346**, 9 (1995).
[15] O. Sorlin *et al.*, Phys. Rev. Lett. **88**, 092501 (2002).
[16] H. Scheit *et al.*, Phys. Rev. Lett. **77**, 3967 (1996).
[17] T. Glasmacher *et al.*, Phys. Lett. B **395**, 163 (1997).
[18] A. Gade *et al.*, Phys. Rev. C **68**, 014302 (2003).
[19] D. J. Morrissey *et al.*, Nucl. Instrum. Methods Phys. Res., Sect. B **204**, 90 (2003).
[20] D. Bazin *et al.*, Nucl. Instrum. Methods Phys. Res., Sect. B **204**, 629 (2003); J. Yurkon *et al.*, Nucl. Instrum. Methods Phys. Res., Sect. A **422**, 291 (1999).
[21] W. F. Mueller *et al.*, Nucl. Instrum. Methods Phys. Res., Sect. A **466**, 492 (2001).
[22] A. Winther and K. Alder, Nucl. Phys. **A319**, 518 (1979).
[23] W. W. Wilcke *et al.*, At. Data Nucl. Data Tables **25**, 389 (1980).
[24] D. Cline, Annu. Rev. Nucl. Part. Sci. **36**, 683 (1986).
[25] S. K. Patra *et al.*, Phys. Rev. C **65**, 054323 (2002).
[26] D. Almehed *et al.*, Phys. Lett. B **604**, 163 (2004).
[27] A. Petrovici *et al.*, Nucl. Phys. **A704**, 144c (2002); Nucl. Phys. **A708**, 190 (2002).
[28] K. Langanke *et al.*, Nucl. Phys. **A728**, 109 (2003).
[29] S. E. Koonin *et al.*, Phys. Rep. **278**, 1 (1997).
[30] K. Langanke *et al.*, Nucl. Phys. A (to be published).